

TSUNAMI MITIGATION EFFORTS WITH pTA IN WEST SUMATRA PROVINCE, INDONESIA

ABDUL MUHARI^{*,†}, FUMIHIKO IMAMURA[†],
DANNY HILMAN NATAWIDJAJA[‡], SUBANDONO DIPOSAPTONO^{*},
HAMZAH LATIEF[§], JOACHIM POST[¶] and FEBRIN A. ISMAIL^{||}

^{*}*Ministry of Marine Affairs and Fisheries, Republic of Indonesia*

[†]*Disaster Control Research Center, TOHOKU University, Japan*

[‡]*Earth Lab, Indonesian Institute of Science*

[§]*Bandung Institute of Technology, Indonesia*

[¶]*German Aerospace Center, Germany*

^{||}*Andalas University, Indonesia*

Accepted 21 June 2010

This paper describes tsunami disaster mitigation in the West Sumatra region with participatory technology assessment (pTA), which promotes direct interaction among member and experts to discuss issues and reach consensus for mitigation through provision of information and knowledge of science and technology. Two areas were examined: Padang, the capital city; and Painan city, a town in southern West Sumatra Province, Indonesia. Tsunami have damaged these areas at least three times: in 1797, a 5–10-m-high tsunami wave height hit the area; in 1833, a 3–4-m-high tsunami came; and in 2007, an 8.4 Mw earthquake generated a local tsunami with maximum wave height of 1.5 m, as observed near Painan. Because of the high level of tsunami risk resulting from its flat topographic conditions, their respective populations of 820,000 people and 15,000 people are developing tsunami mitigation efforts with support of national institutions and international experts. These cities had different starting points and approaches. Efforts were introduced to produce official tsunami hazards maps. Insights from these lessons and ideas arising from the ongoing process after the 2007 South Sumatra and 2009 Padang earthquakes are discussed herein.

Keywords: Tsunami disaster mitigation; pTA; tsunami model.

1. Introduction

Participatory technology assessment (pTA) is considered a promising means to promote direct interaction among members of the public, interest groups, professional experts, and policymakers in multistakeholder environments with the main aim of including science and technology democratically into governance. Over the last decade, pTA has been applied worldwide, especially in the fields of biotechnology [Joss, 2000]. Implementation of pTA for the field of disaster management, with some adjustments, is new.

The impact of natural disasters, especially tsunami, will have implications for local people in many respects: social, economic, and environmental. It is necessary to

encourage scientific experts, interest groups, local people, and policymakers to communicate and formulate future tsunami mitigation efforts in the region. Kiba [2000] reported that the significance is “visualization of the issue” by the community. From this perspective, efforts of this type can minimize the gap of knowledge either among the community itself, the community and the experts, and among the experts (in this case, i.e., between natural scientist and social scientist) as suggested by Imamura [2009]. On the other hand, efforts of this type can provide local government with a strong knowledge basis for disaster management policymaking in the region because it gives the scientific community a wider space to contribute to policymaking.

Four steps are used in implementing the pTA methodology. First is the consensus workshop, which aims to pose key questions by the member of citizen (lay people) and receive answers from the panel of experts, in order to enrich and expand the debate between experts, policymaker, and interested parties by communicating citizen’s view on potentially controversial technology; the second is the scenario workshop, which aims to formulate a shared vision and to create a basis for action in the region. The third step is the decision conference, which is aimed to present the issues underlying conflict over the disputed issue to the voters, and which is aimed at revealing the distribution of votes and opinions to promote the public debate. The last step is a public hearing attended by local government, politicians, and community about problems that must be solved in the region.

The main aims of this paper include describing past measures, ongoing efforts, and future mitigation plans by implementing the pTA methodology for both areas from the perspectives of national government and international experts. The process of development of the official hazard map in Padang city through the consensus workshop, and on the other hand, the following actions of the mitigation policy based on pTA procedures in Painan are discussed herein.

2. Overview of the Area

Padang, West Sumatra province’s capital city, overseeing a total administrative area of 694.69 km², although the populated area is only 29% of the total (205 km²); and the remaining land area (489 km²) comprises hilly areas with many rivers. With average topographic height of 3 m, the populated area is inhabited by 819,740 people [BPS, 2006]. After the 2004 Indian Ocean tsunami, Padang attracted international interest for its disaster preparedness, because it was predicted as an area confronting earthquake and tsunami threats.

About 90 km south from Padang city is Painan — the capital city of the Pesisir Selatan/Southern Coast District — which is inhabited by 15,000 people (Fig. 1). In the central city of Painan, the total populated area is not more than 4 km². Facing the Indian Ocean in the western part, the flat topographic city is surrounded by hills in northern, southern, and eastern areas. These hills provide higher ground to evacuate people in the case of tsunami.

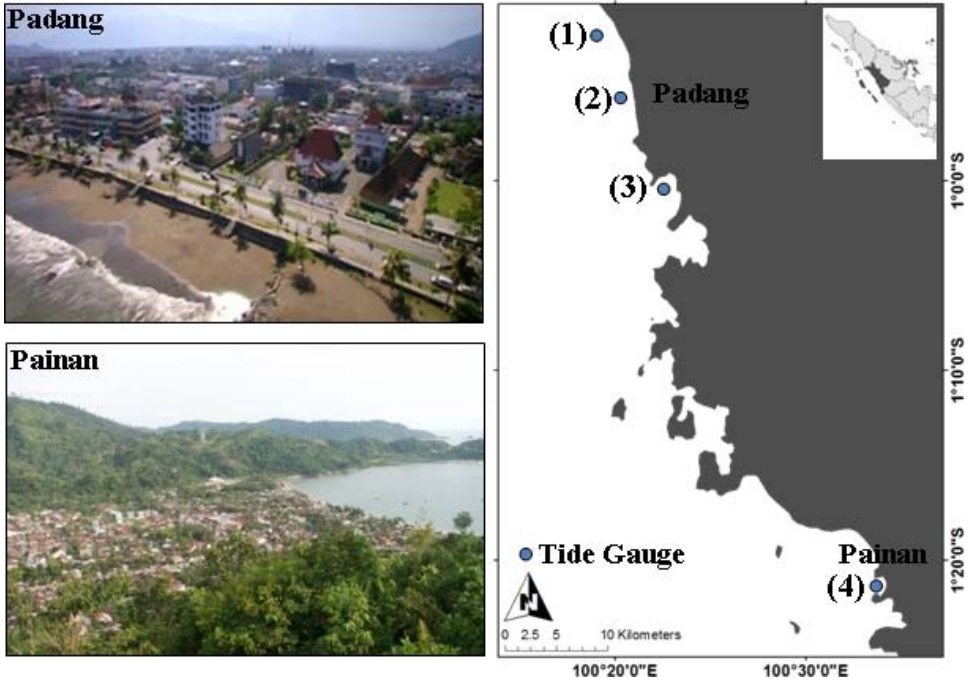


Fig. 1. Study area, Padang and Painan city (left-hand side), the reference tide gauges (center) for modeling at Parupuk Tabing Village (1), Purus Village (2), Teluk Bayur (3), and Painan city (4). Inset figure in the right-hand side is the position of West Sumatra Province (dark gray) in Sumatra Island.

Between the Sumatra subduction zone's front and the cities of Padang and Painan, Mentawai Islands can function as a natural barrier if there are tsunami sources generated on the west of the Mentawai. However, between the islands and the cities of Padang and Painan, it is a large ocean basin with 1750 m depth that has potential for the occurrences of submarine landslides triggered by earthquakes, as suggested by Permana *et al.* [2008].

3. Earthquake and Tsunami Hazard

The cities of Padang and Painan lie in the western part of Sunda Arc region, which extend over 5600 km between the Andaman Islands to the northwest and the Banda Arc to the east. Interplate motion is normal to the arc near Java and becomes oblique at Sumatra [Newcomb and McCann, 1987], the Indian (Indo-Australian) plate converging about 50–60 mm/year toward Sumatra margin on the Eurasian Plate [Sieh and Natawidjaja, 2000]. In 1797, an earthquake with magnitude from 8.5 to 8.7 Mw triggered tsunami with 5–10 m wave height along the coast [Natawidjaja *et al.*, 2006]. Thirty-six years later, in 1833, another earthquake with magnitude 8.6–8.9 Mw occurred in the southern part, overlapping with the previous

one [Subarya et al., 2006], triggered a tsunami over 550 km along the south central coast of Sumatra, with estimated wave height of 3–4 m in the Padang coast [Natawidjaja et al., 2006]. In February 1861, an earthquake of 8.3–8.5 Mw triggered a tsunami with 7 m maximum wave height observed in Nias Island. It affected about 500 km of North Sumatra coast [Newcomb and McCann, 1987].

Focusing on the Sumatra fore arc region, earthquake continues their threat by releasing energy in 1935 (7.7 Mw) and 1984 (7.2 Mw) [Rivera et al., 2002]. These earthquakes occurred in between the 1861 and 1797 ruptures. Recent tectonic activities in the region started when a 7.9 Mw earthquake occurred just near the southern edge of 1833 rupture area on 4 June 2000 (Fig. 2); this earthquake comprised at least 35% of the total moment of the 1833 earthquake [Abercrombie et al., 2003]. The biggest event in this area occurred in December 2004, 2 years after the 7.3 Mw event in 2002 that occurred below the Simelue Island. The 2004 event (9.3 Mw) produced a powerful ground shaking with duration between 8.3–10 min, generating a transoceanic tsunami with wave height up to 30 m. This event claimed more than 2,30,000 casualties in at least 11 countries. The recorded earthquake epicenter is located in the northern part of Simelue Island, but the rupture propagated northward to the Andaman Islands region, producing a giant fault rupture with

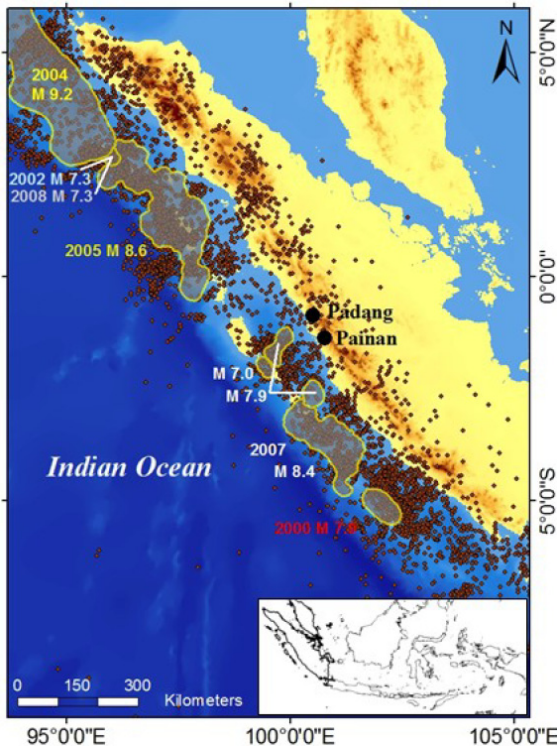


Fig. 2. Seismic rupture in Sumatra region since 2000. (Inset) Sumatra Island (bold) in Indonesia region.

1300 km length along the northernmost section of the Sunda subduction zone. This 2004 earthquake shed stresses to the nearby section in the region beneath the island of Simelue and Nias, resulting in a 8.7 Mw earthquake that occurred only 3 months after. The 2005 event also caused widespread destruction in the islands and claimed at least 2000 victims [Nalbant *et al.*, 2005].

The series of megathrust earthquakes in Sumatra fore arc region continues. In September 2007, within 12 h, two earthquakes occurred in southern Sumatra fore arc region, just next to the 2000 rupture. First mainshock with 8.5 Mw triggered a tsunami with a maximum run-up height up to 5 m [Borrero *et al.*, 2009]. The second, largest aftershock (7.9 Mw) hit on the same day (UTC time), generating tsunami with maximum run-up height up to 1.5 m, observed in Air Haji village, near Painan region (Southernmost of West Sumatra Province) [MoMAF, 2007]. The rupture areas of these earthquakes are within the 1833 rupture zone. However, the moment release by these events is only a fraction of the 1833 event; by calculation, it was not more than 25% of the moment deficit that had accumulated since 1833 [Konca *et al.*, 2008].

After the 2007 events, a big seismic gap is lying in front of West Sumatra Province. A comprehensive studies of geodetic (GPS) and paleogeodetic from microatoll suggest that the gap has potential to fail in the near future and produce a megathrust earthquake with estimated magnitude of 8.6–8.9 Mw [Sieh *et al.*, 2008; Natawidjaja *et al.*, 2009]. Therefore, an integrated effort in order to mitigate future predicted catastrophe must be undertaken in this area.

In this paper, tsunami hazard is evaluated using the worst scenario that can be used for further planning purposes in disaster management. Two different tsunami scenarios were applied in Padang and Painan. These two areas basically will be affected by the same tsunami scenario. However, different times of the research, along with the development of the several models of the future tsunami-source scenarios based on progressively incoming new data, as well as different concepts, coupled by sequence of large earthquake events in the region have altered and improved the prediction of future tsunami source affecting both areas. For example, when we conducted the tsunami hazard assessment in Painan at the beginning of 2007, we used the earthquake source model of the 1797 event from Natawidjaja *et al.* [2006] for as possible worst scenario from historical earthquake perspective. Then, after the 2007 earthquake in Southern Sumatra region, Chlieh *et al.* [2008] predicted future earthquake source based on the moment deficit in Mentawai megathrust. The result of this study was then confirmed by Konca *et al.* [2008] taking into account the 2007 event. Natawidjaja *et al.* [2009] then made more detail evaluations to formulate a scenario for future tsunami source in West Sumatra which is discussed furthermore in hazard assessment at Padang city. Referring to the main aims of the hazard assessment on this paper, we seek reliable values and more conservative values of future predicted tsunami event's parameters to accommodate planning needs for mitigation. The most reliable values can describe the real characteristics of tsunami in the region. Moreover, values that are more conservative are useful for planning and design of structural mitigation in the region.

4. Implementation of Participatory Technology Assessment

4.1. Padang case

National tsunami drill events were started 1 year after the 2004 Indian Ocean tsunami. The awareness of the local government and the community of Padang city rose as international researchers frequently mentioned that Padang city is vulnerable to earthquakes and tsunamis, as noted by McCaffrey [2007], Sieh [2006], and McCloskey *et al.* [2009]. Continual efforts by local NGOs together with local university and respective government institutions are intended to improve community awareness by conducting activities such as placing understandable hazard maps, teaching disaster preparedness in school, sponsoring awareness campaigns, developing a strategic plan for disaster management, awareness campaign, and producing standard operational procedures for emergencies, along with the construction of earthquake-resistant bridges in priority areas. A pilot project for community-level disaster preparedness has already been launched and supported by various national and international parties [Kogami, 2008].

Concurrently, various scientific efforts for tsunami hazards and vulnerability assessment were conducted by many parties. They can be summarized as follows: Ministry of Marine Affairs and Fisheries use the same level approximation with the Global SRTM data on 2006 [MoMAF, 2006]. Borrero modelled inundation based on events in 1797, 1833, and some combination event possibilities for the worst case in 2006 [Borrero *et al.* 2006]. The Indonesian Volcano and Geological Disaster Mitigation Agency in 2008 produced a numerical model based on historical events and possible stress accumulation in the region. The German–Indonesia Tsunami Early Warning (GI-TEWS) project developed a tsunami early warning system, and created an inundation map based on the hazard probability derived from hundreds of scenarios to avoid underestimation of the predicted worst case in 2008, and Hanover University produced an inundation model using high-resolution topography and bathymetric data in 2008 [Goseberg and Schlurmann, 2008]. However, different estimation of the tsunami source, in addition to different bathymetric and topographic data that were used on numerical model produced significant differences in the numerical results. The absence of an official hazard map generates confusion for local governments in preparing a mitigation plan for formulating the policy, budgeting, spatial planning, and permission related to the development of coastal areas.

4.1.1. Effort to make official hazard map

To gain the maximum benefit of the ongoing momentum in tsunami disaster risk-reduction initiative in Indonesia especially in Padang, a case study is necessary in developing an official tsunami hazard map for local government in the form of a technical and community participation workshop. Producing tsunami hazard map is a multidisciplinary process that necessitates the involvement of many scientists

with background in tsunami modelling, seismic, oceanography, and GIS/mapping. More importantly, the community must be involved in the process to verify local and site-specific conditions. Considering those matters, the initiative to have a consensus workshop arose. This initiative will facilitate different methods and results from different agencies and experts to create an official tsunami hazard map for use by the local governments, communities, and the private sector. The first consensus workshop on developing the official hazard map in Padang was held on 25 August 2008. At this workshop, panels of experts reviewed several available results on tsunami hazard assessment in Padang city from local NGO, local government, national government and international experts, and other interest groups, presenting their findings using various data and methodology. University students and local NGO are subjected as lay panel. From this workshop, all participants agreed that Padang city requires an official hazard map that is scientifically accountable and which is useful as a reference for tsunami disaster preparedness. Furthermore, other issues clarified in this workshop were the needs of reliable tsunami source in the region will be fulfilled by the work of Natawidjaja *et al.* [2009]. On the other hand, identical bathymetric accuracy and topographic data should also be used to support numerical calculations. After all related parties have produced results based on the conditions listed above, the official hazard map can be finalized in the decision conference and during public hearings.

In order to support the development of the official hazard map as mentioned above, we first review some available tsunami source information to determine the worst case in terms of arrival time and observed tsunami wave height at given reference tide gauges (Fig. 1). We then modelled respective scenarios using three types of run-up models to assess worst-case inundation parameters such as inundation length, flow depth, wave pressure, flow velocity, and direction. This is directed to assessment of the possible result that might arise from the available run-up methodology and its limitations in predicting inundation characteristics. Finally, we summarize findings into recommendations for tsunami hazard assessment methodology in Padang, Indonesia.

4.1.2. Tsunami source and propagation model

Scenarios based on results reported by Chlieh *et al.* [2008], Natawidjaja *et al.* [2009], Aydan [2008], and Tobita *et al.* [2007] (called scenarios (a)–(d) hereinafter refer to Table 1) modelled using Okada theory [Okada, 1985]. For scenarios (a) and (b), a sophisticated inhomogeneous slip distribution is presented. The slip accumulation of the current locked zone at Mentawai Patch [Sieh *et al.*, 2008] is explained by 348 fault subsets with $20 \text{ km} \times 20 \text{ km}$ dimensions. There were two scenarios proposed by Natawidjaja *et al.* [2009] for the future possible scenarios based on slip accumulation in the region, one is the moderate case that led to an 8.8 Mw and the worst case led to 8.92 Mw. In this paper, we focus on scenario (b) using the worst case scenario (8.92 Mw). The fault subsets in scenarios (a) and (b) are calculated

Table 1. Fault parameter of modeled source scenarios.

ID	Source model	Fault number	Slip (m)	Length (km)	Width (km)	Strike (°)	Dip (°)	Rake (°)	Depth (km)
a	Chlieh <i>et al.</i> [2008]	1	0.3	20.0	20.0	325.0	13.0	75.0	8.5
		2	0.6	20.0	20.0	325.0	13.0	75.0	8.5
	
		348	2.1	20.0	20.0	325.0	13.0	75.0	58.0
		1	0.5	20.0	20.0	325.0	13.0	75.0	8.5
b	Natawidjaja [2009]	2	0.9	20.0	20.0	325.0	13.0	75.0	8.5
	
c	Aydan [2008]	348	3.1	20.0	20.0	325.0	13.0	75.0	58.0
d	Tobita [2007]	1	6	450	117	325.0	13.0	75.0	10.0
		1	7	370	125	325.0	13.0	75.0	10.0

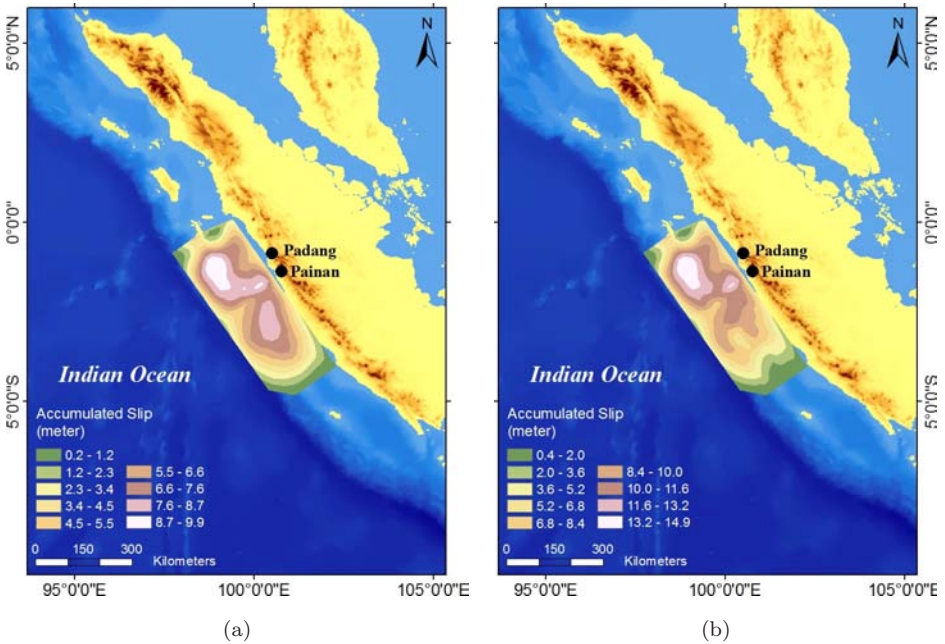


Fig. 3. Description of slip accumulated on scenario (a) on the left-hand side and scenario (b) on the right-hand side.

simultaneously without any consideration of the rupture speed. We only put a few detailed description of the fault subsets (a) and (b) in Table 1, since more complete definition about the slip accumulation distribution is presented in Fig. 3

For scenarios (c) and (d), we only have information about potential magnitude and the prediction of fault length. We assumed that the predicted faults are simple rectangular fault. Therefore, an empirical relation described by Papazachos *et al.* [2004] was used to determine the fault dimensions and dislocations from the predicted magnitude. Other parameters were assumed as the fault characteristics in

the region. We obtained different estimation for fault dimensions for scenarios (c) and (d). For example, we obtained only 395 km fault length in case (c), although it suggests a 450 km fault length in the reference. We calculated 446 km fault length in case (d), although it suggests only a 370 km fault length in the reference. An adjustment for this parameter is performed to satisfy the respective references, without significantly changing the moment magnitude resulted from the adjusted fault parameters.

For comparison of the results, two other available scenarios were those of Borrero *et al.* [2006] and McCloskey *et al.* [2007] which presented results for arrival time, tsunami wave height in the coast [McCloskey *et al.*, 2007], and also inundation zone [Borrero *et al.*, 2006].

To obtain the wave height and arrival time parameters in the given reference tide gauges, the propagation of initial sea surface height as tsunami source was then modelled using a set of nonlinear shallow water equations in the TUNAMI N2 model as it is given below:

$$\frac{\partial \eta}{\partial t} + \frac{\partial M}{\partial x} + \frac{\partial N}{\partial y} = 0 \tag{1}$$

$$\frac{\partial M}{\partial t} + \frac{\partial}{\partial x} \left[\frac{M^2}{D} \right] + \frac{\partial}{\partial y} \left[\frac{MN}{D} \right] + gD \frac{\partial \eta}{\partial x} + \frac{gn^2}{D^{7/3}} M \sqrt{M^2 + N^2} = 0 \tag{2}$$

$$\frac{\partial N}{\partial t} + \frac{\partial}{\partial x} \left[\frac{MN}{D} \right] + \frac{\partial}{\partial y} \left[\frac{N^2}{D} \right] + gD \frac{\partial \eta}{\partial y} + \frac{gn^2}{D^{7/3}} N \sqrt{M^2 + N^2} = 0 \tag{3}$$

$$M = \int_{-h}^{\eta} u \, dz, \quad N = \int_{-h}^{\eta} v \, dz, \quad D = h + \eta \tag{4}$$

In those equations, M and N respectively signify the discharge flux in the x and y directions; η denotes water elevation, and h represents the water depth.

A reference tide gauge was placed in Padang coast at 5 m depth at the Parupuk Tabing coast (1) and at Purus (2) and Teluk Bayur (3). One tide gauge was placed in Painan city (4) at 11 m depth. To compute the tsunami arrival time and maximum wave height in the coast, we used the 1-arc-minute digital bathymetric grid (GEBCO) data. The initial sea surface distribution from respective scenarios is given as Fig. 4.

Numerical calculation with a 1 s time step and 2 h simulation time gives a clear tsunami propagation characteristic spatially and also in time series. From the results at the reference tide gauges (Fig. 5), a similar wave pattern in terms of period was shown for scenarios (c) and (d). Average arrival times in these cases were 34.5 min for (c) and 32.9 min for (d). Different fault dimensions in the single fault scenario, brings a slight difference on its arrival time and significant difference on the wave height. For scenarios (a) and (b), a slightly different wave period and significantly different wave height were also visible. Average tsunami arrival times for scenarios (a) and (b) were faster than those of two other scenarios (c) and (d), and also with other previous result in the region — Borrero *et al.* [2006] for all cases and

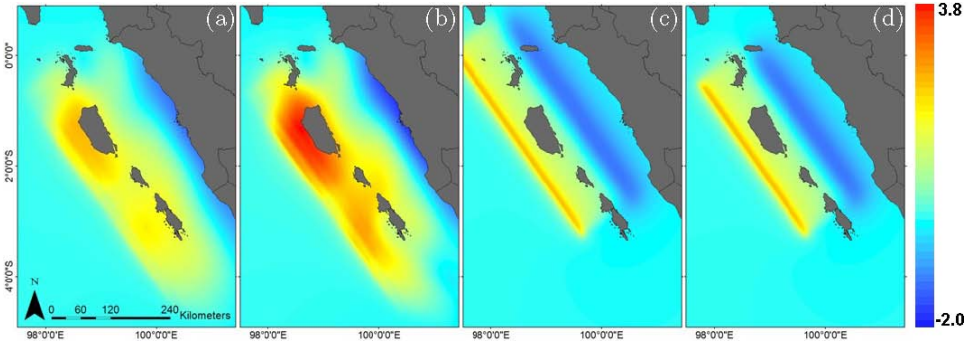


Fig. 4. Initial sea surface distribution of modeled source scenarios.

McCloskey *et al.* [2007] for all cases. Scenario (a) or (b) — showed the average arrival time as only 21 min in the Padang area, and 22 min in the Painan area. For all cases, Borrero *et al.* [2006] shows that the average tsunami arrival time is around 35 min, and McCloskey *et al.* [2007] reports the average tsunami arrival time as 33.5 min. However, these two previous results have closely matching average tsunami arrival times resulted from scenarios (c) and (d), which is 34.5 and 32.9 min, respectively. Especially for scenario (c), because it gives some calculation result based on empirical relation, the average maximum wave height from the empirical equation in the reference [Aydan, 2008] is 11 m while the result from numerical simulation is only 5.8 m in bay area (reference tide gauge number 3). The tsunami arrival time for this scenario shows a significant difference from the result from the empirical equation as well. The numerical simulation shows that the average arrival time is 34.5 min, although the empirical relation on the reference yields 58 min. Further analysis in this paper will use the result from numerical analysis. In general, the highest tsunami is indicated by the first wave from the scenarios (a) and (b), and by the second wave for scenarios (c) and (d) in the Padang area, as shown in Table 2. In the Painan area, the third waves of scenarios (c) and (d) indicate the maximum wave height: they are as high as 7.2 m for (c) and 8.9 m for (d).

The results presented above elicit several impressions. First, possibilities for future tsunami events derived from predicted seismic gap with a maximum wave heights of 3.1–10.7 m exist depending on the location along the coast. Second, the tsunami arrival time might be faster than the previous calculation because of some improvement on crustal deformation research in the region, which implies the possibility of deriving the slip distribution of future predicted earthquake, as given by scenarios (a) and (b). Consequently, the worst scenarios in terms of arrival time are scenarios (a) and (b), with only 21 min on average. The maximum tsunami wave height shown by scenario (b) indicates that this scenario is the worst of all possible scenarios. This scenario then will be used to analyze the inundation characteristics in Padang city, especially at the central part of Padang.

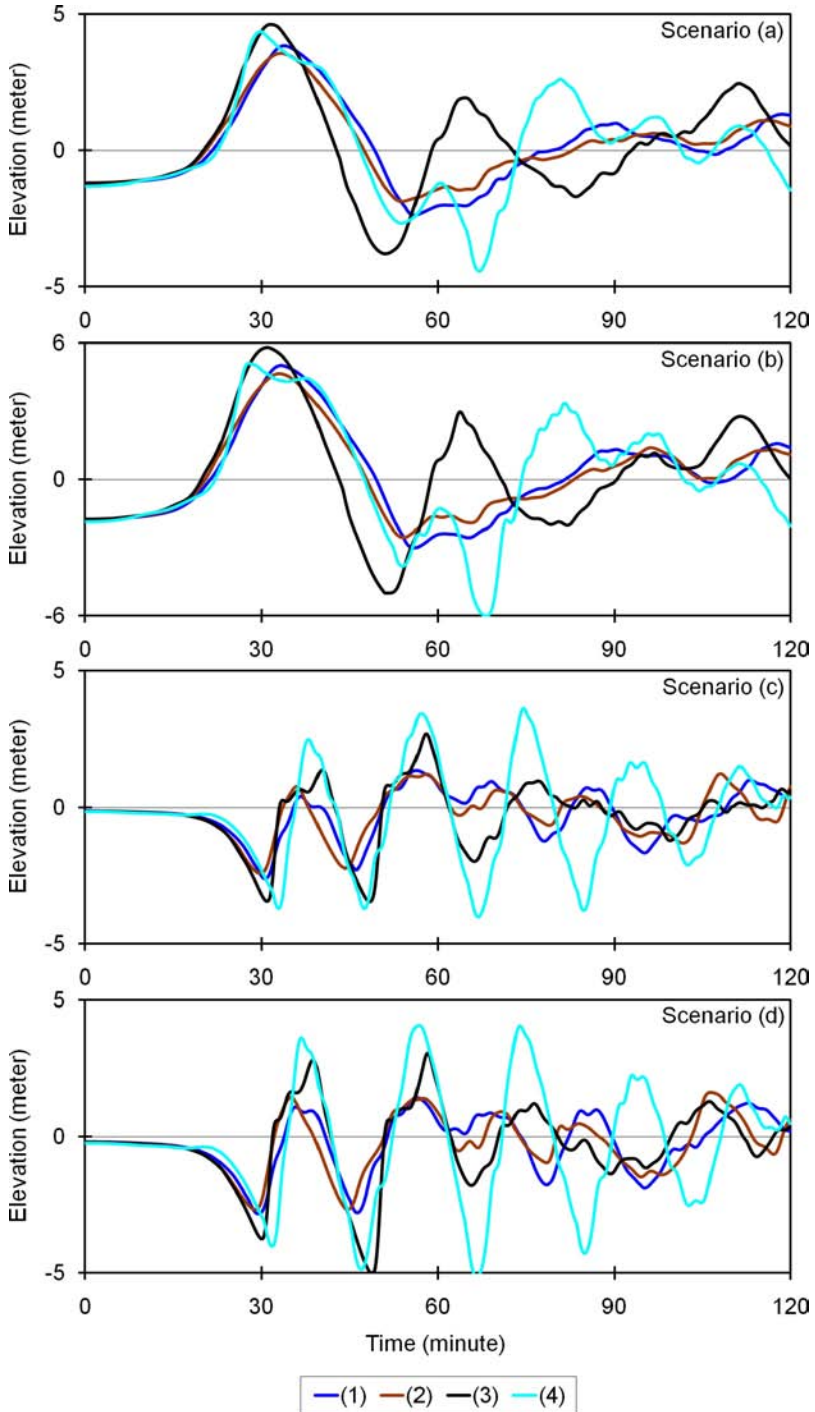


Fig. 5. Time series of tsunami wave in the reference tide gauges (color indicate the respective number of tide gauges that refer to Fig. 1, and scenarios (a), (b), (c), and (d) refer to Table 1).

Table 2. Arrival time and maximum wave height observed at the tide gauges, Numbers (1), (2), (3), and (4) are the tide gauges that refer to Table 1.

ID	Source model	Arrival time (min)				Max. wave height (m)			
		(1)	(2)	(3)	(4)	(1)	(2)	(3)	(4)
a	Chlieh <i>et al.</i> [2008]	22.0	20.8	20.0	22.6	6.0	5.3	8.2	6.8
b	Natawidjaja [2009]	21.6	20.5	20.0	22.3	7.9	7.1	10.7	8.7
c	Aydan [2008]	35.5	33.6	33.1	35.8	3.1	3.1	5.8	7.2
d	Tobita [2007]	33.7	32.0	31.8	34.2	3.8	3.7	7.8	8.9

4.1.3. *Tsunami inundation model*

We modelled tsunami inundation in central Padang using three types of run-up models. First are run-up models with similar roughness coefficients [Imamura, 1996]; second are run-up model with building features (area and height) [Hong, 2004]; the last are run-up models with distributed roughness (equivalent roughness model) [Aburaya and Imamura, 2000]. To calculate the respective run-up models, the model domain is divided into five subdomains (Fig. 6) to fulfil the nested system requirement, a Kriging interpolation is performed for data in the largest domain to avoid

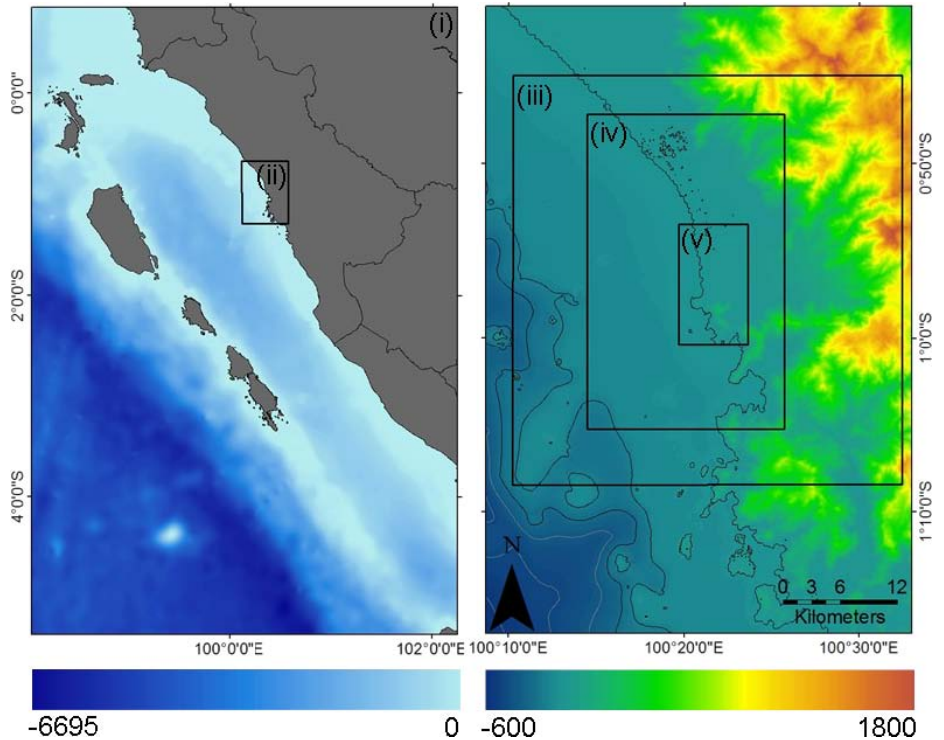


Fig. 6. Computational domain for the model of tsunami propagation and inundation in the city of Padang. The grid size varies from 405 m (i), 135 m (ii), 45 m (iii), 15 m (iv), and 5 m (v), in a nested grid system.

changing the data accuracy in the smallest domain. The domain cell size varies from 405 m to 5 m. The GEBCO set data distributed by British Oceanographic Data Centre [1997] is combined with bathymetric data obtained from the Ministry of Marine Affairs and Fisheries with 200 m accuracy in the larger domain. Surface and terrain topographic data with 5 m accuracy (DLR, 2008a) are used to compute tsunami inundation in smallest domain, as shown in Fig. 7. Careful digitations are performed to adjust the accuracy of bathymetric data in the smallest domain to produce a set of topographic and bathymetric data with 5 m accuracy.

For the run-up model with similar roughness, we use a 0.025 roughness coefficient in the whole domain. In the run-up model with a building feature, building height information obtained from surface topography data directly puts in the topographic domain (DLR, 2008b). On the other hand, in the run-up model using the distributed roughness coefficient, we used the value of roughness coefficient as shown in Table 3. In this method, for densely populated areas, we used a resistance law based on the equivalent roughness coefficient given by Aburaya and Imamura [2000] as shown in Eq. (5):

$$n = \sqrt{n_0 + \frac{C_D}{2gd} + \frac{\theta}{100 - \theta} \times D^{4/3}} \quad (5)$$

Subscript n_0 is the Manning roughness coefficient (0.025), θ is the building/house occupancy ratio in the smallest grid (5 m), C_D is the drag coefficient (1.5), d is the horizontal scale of the house measured using GIS data, and D is the modelled flow depth. Manning's roughness coefficient was obtained from Kotani *et al.* [1998].

To determine the land use features, we used land use data derived from satellite image processing (DLR, 2008c) to create the roughness domain as well as the building occupancy domain (Fig. 7). We use the same grid size (5 m) in the smallest domain for all the run-up methodology. This size can represent land features, such as building shape and land occupancy, without changing the original topographic data. All run-up models were calculated under a 0.05 s time step for 2 h calculation time.

Calculation results show different roughness and building features in topographic data has a significant influence on estimating inundation zone (Fig. 8). To compare and analyze these models' results in a densely population area, we used three control points; two of them are placed on land and one in the river (below Siti Nurbaya Bridge). We put a control point below the Siti Nurbaya Bridge to estimate the reliability of the bridge for use as a proposed shelter location in the case of tsunami. The other three cross-sections are perpendicular to the shoreline up to 100 m landward to check the behavior of tsunami inundation in coastal areas, as given in Fig. 9. The resultant time series from three run-up models in respective control points and cross-section inundation depth are shown in Figs. 10 and 11.

The run-up model with building feature and distributed roughness gives a smaller inundation area than the run-up model with similar roughness coefficient.

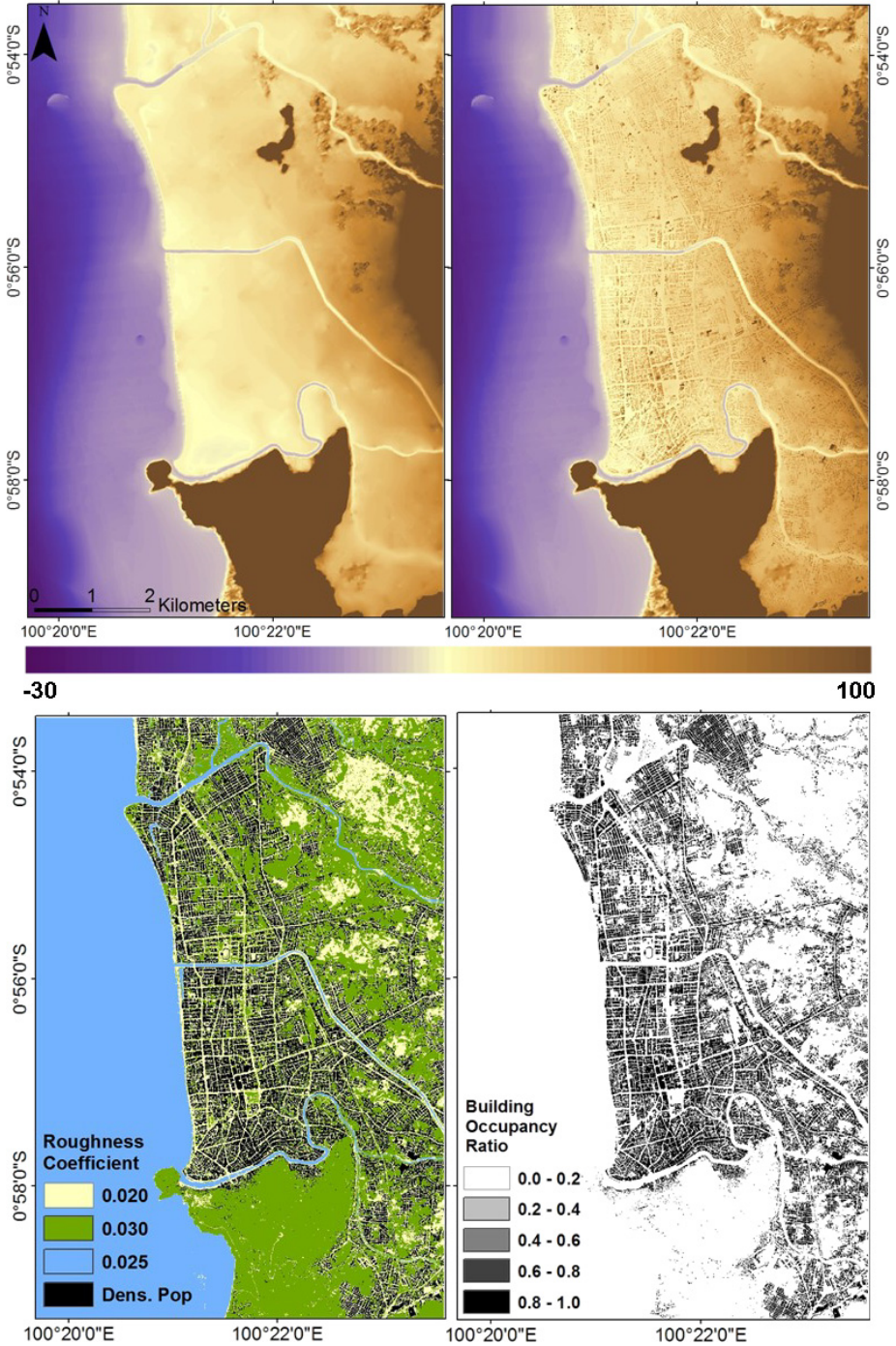


Fig. 7. Topographic data (top) for run-up model with similar roughness (left), and building feature (right). Land use data (bottom, left) and building occupancy ratio (right) for run-up model with distributed roughness.

Table 3. Values of manning roughness coefficient [Kotani *et al.*, 1998].

Land cover	n
Smooth ground	0.02
Vegetated area	0.03
Shallow water	0.025
Populated area	0.045
Densely populated area	Eq. (5)

The run-up model with building features shows real conditions of tsunami flow through the buildings, and undergoes resistance when it hits them. Such a resistance effect, especially for tsunami flow velocity, can be described also by the distributed roughness model. However, it fails to show the decreasing inundation depth in the front side or back side of buildings as well as the flow increase when it passes through a narrow road, as shown in Figs. 10(I) and 10(II). Missing dotted lines (red) in Figs. 10(I) and 10(II) show the existence of buildings. This result is consistent with results obtained by Hong and Imamura [2004] related to the comparison between the use of the distributed roughness model and the topographic model with building features in urban areas.

From the observed inundation time series at given control points, the run-up model with distributed roughness coefficient reaches the respective point with longer arrival time and lower run-up height (Figs. 11(a) and 11(b)). This can be understood because the respective control points are put at a junction of narrow roads. The existence of buildings along the road makes the velocity and run-up height becomes greater than the surrounding areas. This effect can be shown more clearly in Figs. 10(II) and 10(III) that the inundation depth of run-up model with building feature (red-dotted line) is higher than the inundation depth by a run-up model with distributed roughness (blue-dotted line) when the cross-section is across the narrow street. Figure 10(II) shows the run-up variability along Raden Saleh Street. When the tracing line crosses the building, then the run-up height will decrease immediately (lower than run-up with distributed roughness). However, when it flows through the road, then the run-up height will increase and become greater than the result from the run-up height with distributed roughness. Below the Siti Nurbaya Bridge, we obtained around 4 m maximum water elevation below the Siti Nurbaya Bridge (Fig. 11(c)), which is still reasonable if it is proposed as a shelter location because the bridge height is around 10 m.

The use of the assumption that all the buildings can survive tsunami force, both a run-up model with building features and the run-up model with distributed roughness might yield underestimations of tsunami inundation length because of the building resistance effect. On the other hand, the lack of building features to reduce the tsunami wave energy in a run-up model with a similar roughness coefficient might cause overestimation because no resistance factor acts on the flow except for the bottom friction with the similar roughness condition.



Fig. 8. Comparison of the result from run-up model with similar roughness (left), run-up model with building feature (center), and run-up model with distributed roughness (right) overlaid on satellite image of Padang city.

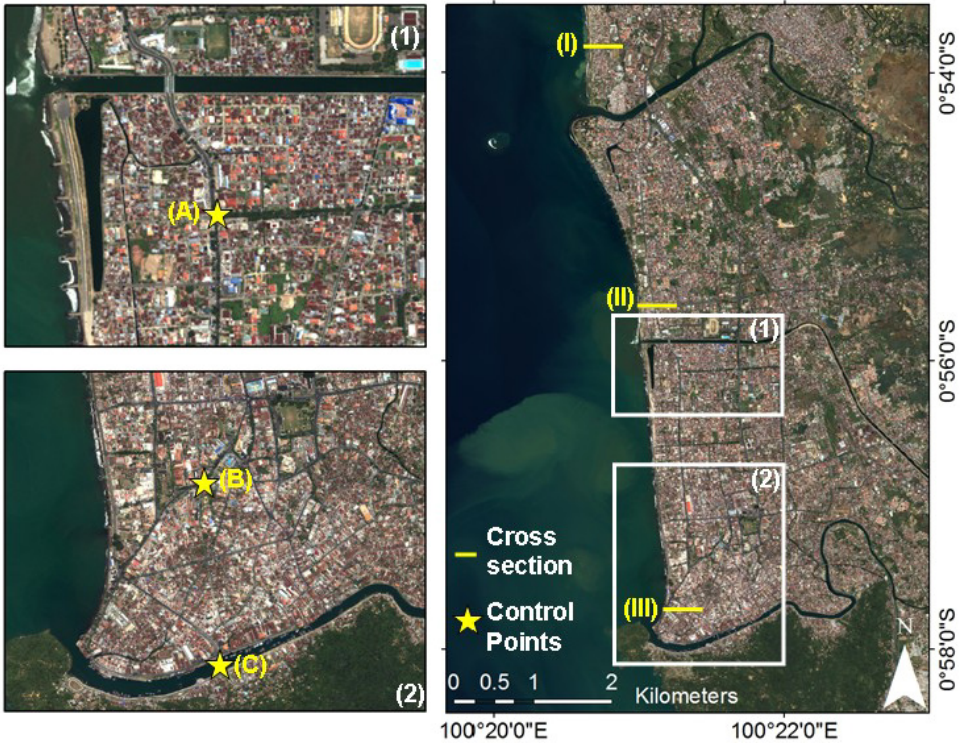


Fig. 9. Control points for time series analysis, (A) Ujung Gurun Street, (B) Bundo Kandang Street, and (C) Below Siti Nurbaya Bridge; Cross-section trace line (I) South part of Parupuk Tabing Village, (II) Raden Saleh Street, and (III) Muara Village.

Even if it does not represent the surge force of a tsunami wave front, the result of the run-up model with a building feature is important to analyze details of the wave pressure distribution and flow velocity as well as its direction. This determines which way should be avoided and which way should be taken in cases of evacuation. The model can suggest the safest road away from tsunami flow from time to time, and which roads will be inundated but which will not disrupt evacuation. Furthermore, the run-up model with building mask is able to predict the potential debris flow from the buildings which may be damaged by the earthquake. The experience of the 2009 earthquake showing that the building in Padang is very prone to ground shaking as it will be explained in the next section.

In the light of the results described above, we can show a run-up model with a building feature or a run-up model with distributed roughness that represents a more realistic inundation zone, rather than a run-up model with similar roughness. However, for a more conservative value, the result of run-up model with similar result can still be considered to give a “buffer” result for planning and engineering design purposes.

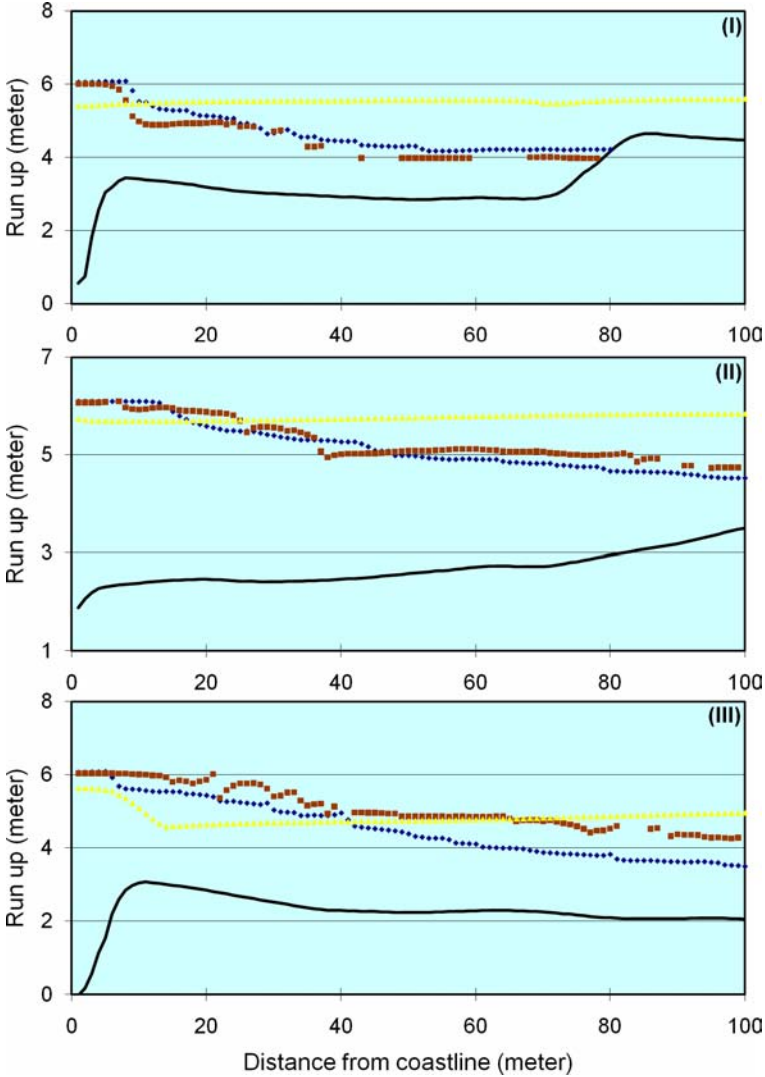


Fig. 10. Cross-section of run up height (I), (II), and (III). Yellow-dotted line is the result from run-up model with similar roughness, brown-dotted line is the result from run-up model with building feature, and blue-dotted line is the result from run-up model with distributed roughness. Black line is the topography of the cross-sections.

4.1.4. *The 2009 earthquake and damage*

On 30 September 2009, a 7.6Mw earthquake in West Sumatra caused massive destruction to buildings and infrastructure in Padang. At least 1,35,448 houses were lost; an additional 65,380 houses sustained medium damage, and 78,604 houses were slightly damaged [BNPB, 2009]. The total economic loss was as much as \$2.15 billion.

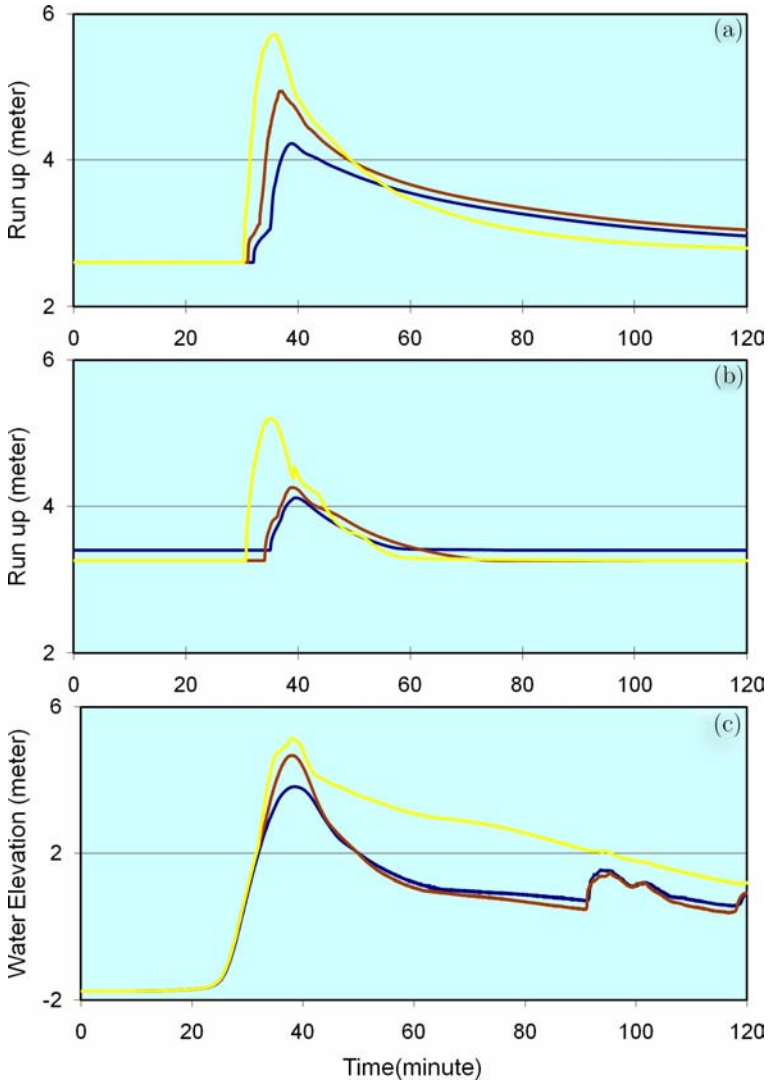


Fig. 11. Time series of run-up height at points (a), (b), and (c). Yellow line is the result from run-up model with similar roughness, brown line is the result from run-up model with building feature, and blue line is the result from run-up model with distributed roughness.

A reconnaissance survey conducted by Tohoku University, the Asian Disaster Research Center (ADRC), and Earthquake Research Institute (ERI) in Padang on 14–16 October 2009, briefly describes conditions of the damage in Padang city and neighboring districts (JST-JICA, 2009).

Damage to buildings caused by vibration, however, was seen in the city of Padang, Pariaman (district in 30 km north of Padang), and in the mountain villages of Padang–Pariaman county (district between Padang city and Pariaman city).



Fig. 12. Three major damage classifications in Padang, damage on reinforced concrete building (left), damage on nonreinforced concrete (center), and damage on ordinary residential houses (right).

Moreover, many landslides occurred in the hilly areas in these districts. Ground liquefaction occurred in some areas but most cases seemed not to be major elements of structural damage.

The damaged buildings were categorized into three groups (JST-JICA, 2009). First were large reinforced concrete frame buildings having three or more storeys (Fig. 12, left-hand side). Many in the city area of Padang were rated as damaged. The concrete strength of some damaged buildings was measured using a simple test method (Schmidt hammer test); the strength was compared to the extent of damage. The strength of the damaged buildings' concrete was mostly of common level; thereby, the main factors of the damage are not caused by the poor workmanship but in the poor structural planning and design. Damage was noted to buildings that had been intended for use in tsunami evacuation in Padang. Five of ten are too damaged to be used for the purpose. The specifications to select the existed one for the evacuation building should therefore be reconsidered. Second was the nonreinforced masonry buildings concentrated in the area designated as Chinatown in Padang (Fig. 12, center). They were 2–3 storey brick masonry structures. Many had been reduced to rubble. The third one is the residential houses constructed using cheap materials and cheap construction methods (Fig. 12, right-hand side). At villages in hilly areas of Padang–Pariaman county, most houses had been made of wood, or stone, and lime mortar walls, with nonreinforced brick pillar or poorly reinforced concrete pillar. They had been damaged severely. Buildings belonging to the second and third were essentially weak against earthquakes. Their improvement requires not only technical approaches but also social and economical approaches.

4.2. Painan case

The effort to make tsunami hazard map in Painan and its follow-up action is more advance in this region. It started with public awareness activity about tsunami hazard conducted in 2006 by the national government. Local authorities then initiated the construction of tsunami evacuation sites. This effort was undertaken in parallel with detailed assessments about tsunami hazards in the city. The workshop

to visualize the idea for mitigation and disseminate the assessment result was conducted twice in this region: first for the local government and the community (in both, their cultural leader and the citizen itself), and second for coastal villagers in the form of cultural activity.

4.2.1. *Tsunami hazard analysis*

A scenario by Natawidjaja *et al.* [2006] was calculated based on the Masinha theory [Masinha, 1981], and tsunami propagation and inundation modelled using the TUNAMI N2 model. Bathymetric data were obtained from the Naval Bureau for Hydro-Oceanography (DISHIDROS, 2005) with several scales from 1:500,000 until 1:25,000. Topographic data were obtained from the shuttle radar topographic mission (SRTM) with 90 m horizontal accuracy and were enhanced by a topographic levelling survey to yield 2.5 m accuracy for the smallest model. The building distribution was digitized manually from QUICKBIRD images [2006], which are used also for hazard map visualization as well. Other data used in this step were geographic-based census data from the Center Statistical Bureau (BPS) [2006] for human vulnerability assessment.

The tsunami source mechanism for the hazard map is modified from Natawidjaja *et al.* [2006] for the 1797 event. The modification was directed to obtain the worst-case scenario for Painan city. Another possibility of tsunami-generation scenarios in the region was stored in a tsunami database model. We produced around 26 possible rupture zones with several possible earthquake magnitudes on each zone. From all the possible scenarios, we chose the worst-case scenario based on its tsunami wave height in the coastline. The fault mechanism of the tsunami source is portrayed in Table 4, with snapshots of tsunami propagation in the large domain shown in Fig. 13.

A detailed inundation model was produced in the smallest domain with 2.5 m grid size. This accuracy is directed to include detailed information of inundation pattern in the central city, which is only around 4 km² wide. Based on results of the detailed inundation model, the tsunami reaches the coastline in 57 min after the earthquake. This result differs markedly from the result obtained from scenarios (a) and (b) in the Padang case. However, as described in Part 3, we conducted research for Painan in early 2007 when the available scenarios were only those from Natawidjaja *et al.* [2006] and Borrero *et al.* [2006]. During the subsequent 2 years, after which we conducted research for Padang, the progress of geodetic and paleogeodetic research had increased considerably to accommodate the high intensity of seismic events in the region. A revision for this calculation might be conducted to enhance the hazard analysis in the Painan region.

Table 4. Focal mechanism for Painan case.

Mw	Epicenter	L (km)	W (m)	Slip (°)	Strike (°)	Dip (°)	Rake (km)	Depth
8.5	99.92417 -1.529	300	100	10.0	325.75°	10°	70°	10

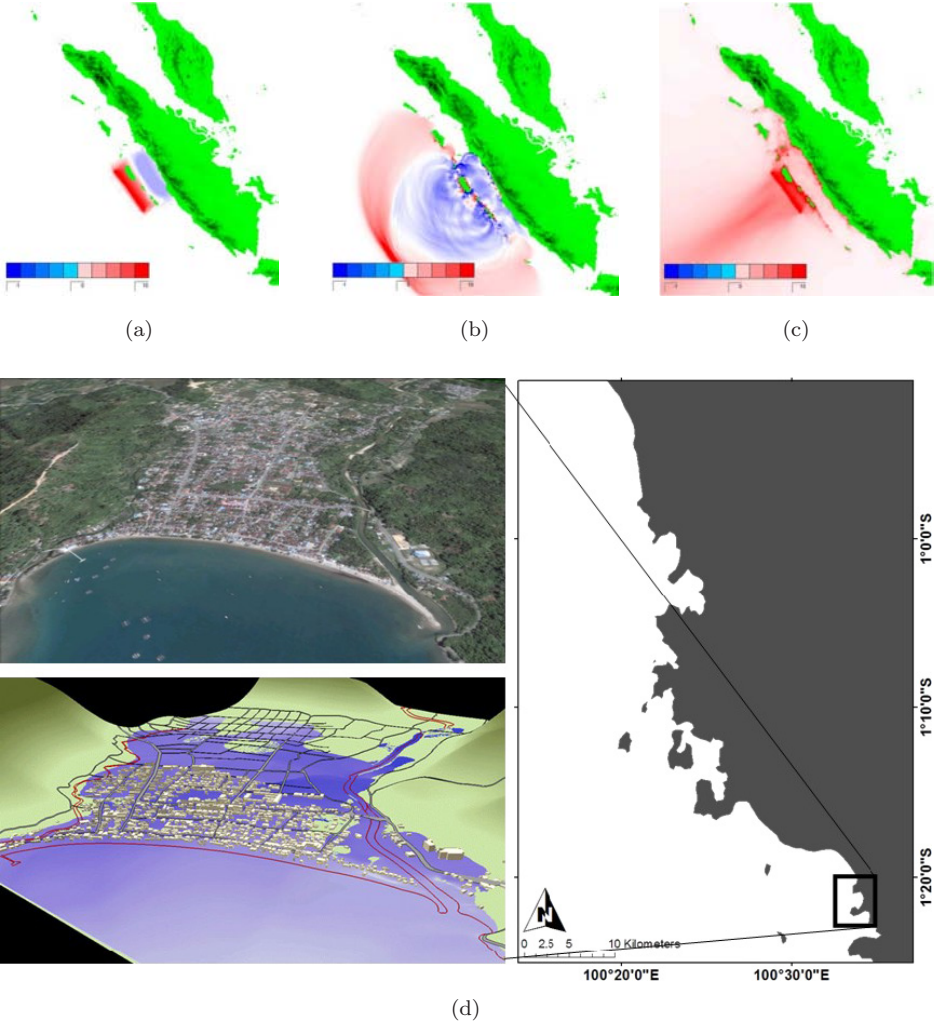


Fig. 13. Result of tsunami simulation. (a) Tsunami generation source, (b) Tsunami propagation after 20 min, (c) Maximum tsunami wave height, (d) Tsunami inundation 96 min after earthquake in a simple three-dimensional visualization.

The maximum inundation depth in the coastal area of Painan is 12 m. This result is reasonable compared with the result from all scenarios in the Padang case. As predicted from the topographic condition, almost the entire city is inundated by the tsunami, only a small area with 6 m elevation in the eastern part of the city survived the tsunami flood. Based on this result, if we assumed that the average normal walking speed for adult people is 1.3 m/s [Thompson and Simulex, 2004], then it could be simply assumed that people from the coastline could reach a safe area before a tsunami comes: the maximum distance from the coastline to evacuation site is only 2 km. To anticipate the evacuation time needed by elderly

people, we determined several evacuation sites near the city center, with average distance of less than 1 km. These can be reached before the tsunami arrives, given the assumption that the walking speed for elderly people is 0.75 m/s [Sugimoto *et al.*, 2003].

4.2.2. Efforts to develop an integrated tsunami disaster mitigation

By adding some critical information such as tsunami evacuation sites and possible evacuation routes within the inundation area, the results from tsunami inundation model were then transferred to the tsunami evacuation map and installed in some priority areas such as a central market, tourism sites, and fishery ports (Fig. 14(a)). To guide the community in case of tsunami, around 348 tsunami evacuation signboards were installed in the designated evacuation site (Fig. 14(b)). Local governments of Painan constructed artificial evacuation sites (Fig. 14(c)) using their respective budgets, demonstrating their concern about tsunami disaster mitigation. The installation of the tsunami evacuation map as well as the tsunami evacuation signboard was finished together with the construction of a tsunami evacuation site



(a)



(b)

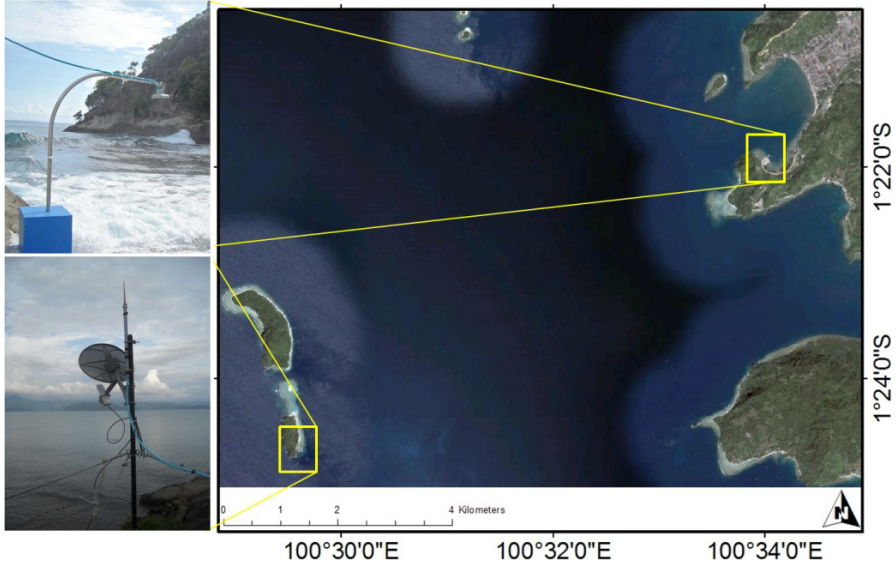


(c)



(d)

Fig. 14. Tsunami countermeasures in Painan city: (a) Hazard map, (b) Tsunami evacuation signboard, (c) Tsunami evacuation site, (d) Tsunami control forest plantation, and (e) Position of installed tide gauges.



(e)

Fig. 14. (Continued)

in mid-2008. Other work finished in 2008 was the planting of coastal vegetation to construct a tsunami control forest in northern Painan city (Fig. 14(d)). The provincial government of West Sumatra supported this work.

The next step in Painan is installing the tide gauge. Fundamentally in the national system, Indonesia has already developed a tidal network to support the national tsunami warning system. However, the installation of a “local tide gauge” in Painan is not intended to be entirely independent from the national system; the local tide gauge is designed to enhance the local capacity for evacuation decisions. For this purpose, two places were chosen for tide gauge placement: the fishery port (Fig. 14(e)) and a small island named Aur Island 11 km distant from the city. A radio with 2.4 GHz frequency sends data from equipment to its computer server. It was chosen because of its capability of sending data up to 56 km with no interference. This radio frequency is also available free of charge to guarantee its sustained use. The time lag of data acquisition by the tide gauge and data visualization on the computer server is only 20s, so probably the tide gauge system provides nearly real-time data.

5. Challenges for Disaster Mitigation

Some insights have been garnered from the ongoing project and latest events in both areas. The first is the need to continue a close assistantship for community preparedness. Focusing on Painan, the construction of such infrastructure has not been followed by an intense community preparedness program. Imamura [2009] suggests

three steps for safe evacuation: appropriate information (official warning) about earthquakes and abnormal phenomena following an earthquake, decision making related to evacuation based on risk perception and previous experience, and selection of a proper route to a safe destination. The first step has already been provided by national and local tsunami warnings; the second and the third steps should be evaluated by conducting frequent community-based evacuation drills to optimize the use of installed infrastructure. Frequent tsunami evacuation drills on a community level will enhance the memory of people in relation to the evacuation route and minimize the time necessary to produce an evacuation decision after receiving a tsunami warning.

In Padang city, although it is known as the city most prepared for tsunami, the damage and huge casualties caused by the earthquake in September 2009 underscore the knowledge gaps that still exist among the populace and scientists, and among social and natural scientists. This event also shows that nonstructural mitigation comprising public education, government policy, drills, and other measures are insufficient without support by implementation of structural mitigation efforts such as strengthening of existing buildings (retrofitting) and construction of evacuation sites, towers, and shelters that are able to resist ground shaking. The latest earthquake, which killed 1200 people, mainly trapped them in low-quality structures. The need to establish building regulations related with earthquake resistance in Padang city is urgent since the 2009 earthquake demonstrates that building quality strongly affects the number of casualties. Damage undergone by nearly 90% of buildings in Padang gives an opportunity to apply this new regulation of building strength.

From experience of at least three earthquakes in 4 years, the city of Padang should consider a community-scale evacuation site, which might be more effective. This strategy can reduce the gap separating people because of the risk bias in terms of decision time by people to make decisions to evacuate after receiving a tsunami warning. The initiation that already developed by local NGO such as KOGAMI [Kogami, 2008] to provide community-scale tsunami disaster preparedness should be supported.

6. Conclusions

A series of earthquakes in the Sumatra fore arc region, consent a big seismic gap which has potential to fail near the future, with estimate magnitude of 8.6–8.9 Mw, emphasizes the threat that is posed to Padang and Painan city.

The first consensus workshop in Padang city provides the recommendation of the needs of the official hazard map, and the technology that should be used on its development. First consensus workshop should be continued after all of related parties conduct assessment as it is required.

From all the possible scenarios derived from existing seismic gap, the scenario proposed by Natawidjaja *et al.* [2009] is the worst scenario in terms of arrival time and maximum tsunami wave height.

Result from all of the run-up models in Padang city shows that maximum flow depth in the coastal area is 6.2 m. The use of run-up model with building feature or run-up model with distributed roughness is able to describe a more realistic tsunami inundation pattern in densely populated area. Application of these models can be used to determine the evacuation route as well as the potential of tsunami debris flow. For design purposes, a more conservative result is needed. This can be provided by the run-up model with similar roughness.

In Painan, complete infrastructure should be balanced by comprehensive community preparedness to optimize the use of respective facilities. Increasing the experience by conducting the evacuation drills will enhance the memory of the community to choose the most appropriate route to evacuate in case of tsunami. Evaluation to assess the effectiveness of the installed equipment should be conducted for further enhancement. Integrated research with implementation oriented will be useful for future mitigation in both areas.

References

- Abercrombie, R., Antolik, M. and Ekstrom, G. [2003] "The June 2000 Mw 7.9 earthquake south of Sumatra: Deformation in the India-Australia plate," *J. Geophys. Res.* **108**(B1), 2018, DOI:10.1029/2001JB000674.
- Aburaya, T. and Imamura, F. [2002] "Proposal of a tsunami run-up simulation using combined equivalent roughness," *Ann. J. Coastal Eng.*, JSCE **49**, 276–280 (in Japanese).
- Aydan, O. [2008] "Seismic and tsunami hazard potentials in Indonesia with a special emphasis on Sumatra Island," *J. School Marine Sci. Technol. Tokai Univ.* **6**(3), 19–38.
- BNPB [2009] Indonesian disaster management body, <http://bnpb.go.id/website>.
- Borrero, J. C., Sieh, K., Chlieh, M. and Synolakis, C. E. [2006] "Tsunami inundation modeling for Western Sumatra," *PNAS* **130**(52), 19673–19677.
- Borrero, J. C., Weiss, R., Okal, E. A., Hidayat, R., Suranto, A. D. and Titov, V. V. [2009] "The tsunami of 2007 September 12, Bengkulu Province, Sumatra, Indonesia: Post tsunami survey and numerical modeling," *Geophys. J. Int.* **128**, 180–194.
- BPS [2006] Indonesian Statistical Bureau, "Village Potential Data," (CD-ROM).
- British Oceanographic Data Centre [1997] "The Centenary Edition of the GEBCO Digital Atlas," (CD-ROM).
- Chlieh, M., Avoac, J. P., Sieh, K., Natawidjaja, D. H. and Galetzka, J. [2008] "Heterogeneous coupling of the Sumatran megathrust constrain by geodetic and paleogeodetic measurement," *J. Geophys. Res.* DOI:10. 1029/2007JB004981.
- DISHIDROS TNI-AL [2005] Naval Bureau for Hydro-Oceanography, Bathymetric map of West Sumatra.
- DLR [2008a] Digital Surface/Terrain Model Padang, version 1. Intermap Federal Service Inc.
- DLR [2008b] Landmask data of Padang.
- DLR [2008c] Landuse data of Sumatra, Jawa and Bali, Version 1.
- Goseberg, N. and Schlurmann, T. [2008] "Relevant factors on the extent of Inundation based on tsunami scenario for the city of Padang, West Sumatra," *Proc. Int. Conf. on Tsunami Warning*, Bali, Indonesia.
- Hong, S. J. and F. Imamura [2004] "Study of the accuracy of the tsunami numerical model around obstacles," *Proc. APAC 2003, Makuhari*, Japan, pp. 18–19.

- Imamura, F., Shuto, N., Goto, C. and Ogawa, Y. [1996] "IUGG/IOC TIME project IOC manual and guides," No. 35.
- Imamura, F. [2009] "Dissemination of information and evacuation procedures in the 2004–2007 tsunamis, including the 2004 Indian Ocean," *J. Earthquake Tsunami* **3**(2), 59–65.
- JST-JICA [2009] "Field survey of the 2009 Padang earthquake, Indonesia," <http://www.eri.u-tokyo.ac.jp/indonesia/resources/091025PadanReport.pdf>.
- Joss, S. [2000] "Participation on parliaments and technology assessment," in Vig, N. J. and Paschen, H. eds., *Parliaments and Technology* (State University of New York Press).
- KOGAMI [2008] Tsunami alert community, <http://kogami.or.id/>.
- Konca, O., Avouac, J. P., Sladen, A., Meltzner, A. J., Sieh, K., Fang, P. *et al.* [2008] "Partial rupture of the locked patch of the Sumatra megathrust during the 2007 earthquake sequence," *Nature* **456**, 631–635.
- Kotani, M., Imamura, F. and Shuto, N. [1998] "Tsunami run-up simulation and damage estimation by using geographical information system," *Proc. Coastal Eng., JSCE* **45**, 356–360 (in Japanese).
- Masinha, L. and Smiley, D. E. [1971] "The displacement field of inclined fault," *Bull. Seismol. Soc. Am.* **61**(5), 1433–1430.
- McCaffrey, R. [2007] "The next great earthquake," *Science* **23**(135), 1675–1676.
- McCloskey, J., Antonioli, A., Piatanesi, A., Sieh, K., Steacy, S., Nalbant, S. S. *et al.* [2007] "Near-field propagation of tsunamis from megathrust earthquake," *Geophys. Res. Lett.* **34**, L14316, DOI:10.1029/2007GL030494.
- McCloskey, J., Lange, D., Tilmann, F., Nalbant, S. S., Bell, A. F., Natawidjaja, D. H. and Rietbrock, A. [2009] "The September 2009 Padang earthquake," *Nature Geoscience* **3**, 70–71.
- MoMAF — Ministry of Marine Affairs and Fisheries [2006] "Tsunami risk assessment in Padang city," Project Report, MoMAF Internal publication.
- MoMAF — Ministry of Marine Affairs and Fisheries [2008a] "Field survey of 2007 Bengkulu Tsunami," Survey Report, MoMAF Internal publication.
- MoMAF — Ministry of Marine Affairs and Fisheries [2008b] "Tsunami risk assessment in Painan city," Project Report, MoMAF Internal publication.
- MoMAF — Ministry of Marine Affairs and Fisheries [2008c] "Design of tsunami vertical evacuation in Padang," Project Report, MoMAF Internal publication.
- Nalbant, S., Steacy, S., Sieh, K., Natawidjaja, D. H. and McCloskey, J. [2005] "Seismology, earthquake risk on Sunda trench," *Nature* **435**(7043), 756–757.
- Natawidjaja, D. H., Sieh, K., Chlieh, M., Galetzka, J., Suwargadi, B. W., Cheng, H. *et al.* [2006] "Source parameters of the great Sumatran megathrust earthquakes of 1797 and 1833 inferred from coral microatolls," *J. Geophys. Res. Solid Earth*, DOI:10.1029/2005JB004025.
- Natawidjaja, D. H., Sieh, K., Kongko, W., Muhari, A., Prasetya, G., Meilano, I. *et al.* [2009] "Scenario for future megathrust tsunami event in the Sumatran subduction zone," *Proc. AOGS Meeting*, Singapore, 2009.
- Newcomb, K. R. and McCann, W. R. [1987] "Seismic history and seismotectonics of the Sunda Arc," *J. Geophys. Res.* **92**(B1), 421–439.
- Okada, Y. [1985] "Surface deformation due to shear and tensile faults in a half-space," *Bull. Seismol. Soc. Am.* **75**(4), 1135–1154.
- Papazachos, B. C., Scordilis, E. M., Panagiotopoulos, D. G., Papazachos, C. B. and Karakaisis, G. F. [2004] "Global relation between seismic fault parameter and moment magnitude of earthquake," *Bull. Geological Soc. Greece* **36**(36), 1482–1489.

- Permana, H., Singh C. H. and Research team [2008] “Submarine landslide and localized tsunami potentiality of Mentawai Basin, Sumatra, Indonesia,” *Proc. Int. Conf. of Tsunami Warning*, Bali, Indonesia.
- Rivera, L., Sieh, K., Helmberger, D. and Natawidjaja, D. H. [2002] “A comparative study of the Sumatran subduction zone earthquake of 1935 and 1984,” *Bull. Seismol. Soc. Am.* **92**(5), 1721–1736.
- Sieh, K. and Natawidjaja, D. H. [2000] “Neotectonic of Sumatran fault, Indonesia,” *J. Geophys. Res.* **105**(B12), 28, 295–28, 326.
- Sieh, K. [2006] “The Sumatran megathrust earthquake: From science to saving lives,” *Phil. Royal Trans. R. Soc. A* **346**, 1947–1963.
- Sieh, K., Natawidjaja, D. H., Meltzner, A. J., Shen, C. C., Cheng, H., Li, K. S. et al. [2008] “Earthquake supercycle inferred from sea-level change recorded in the coral of West Sumatra,” *Science* **322**, 1674–1677.
- Subarya, C., Chlieh, M., Prawirodirdjo, L., Avouac, J. P., Bock, Y., Sieh, K. et al. [2006] “Plate-boundary deformation associated with the great Sumatera-Andaman earthquake,” *Nature* **440**, 47.
- Sugimoto, T., Murakami, H., Kozuki, Y. and Nishikawa, K. [2003] “A human damage prediction method for Tsunami disaster incorporating evacuation activities,” *Natural Hazards* **29**, 585–600.
- Takao, Kiba [2000] “A consideration on the formation process and social meaning of consensus conference,” *J. Sci. Policy Res. Management* **15**(2), 122–131.
- Thompson, P. [2004] “Simulex: Simulated people have needs too,” *NIST Workshop on Building Occupant Movement during Fire Emergency*, NIST, 1–10.
- Tobita, M. [2007] “Crustal Deformation of 2007 Southern Sumatra Earthquake Observed by SAR Interferometry,” Paper presented at DPRI Kyoto workshop, 2008, http://www.rcep.dpri.kyoto-u.ac.jp/~hasimoto/Manabu/InSAR_WS2008/Presentation/Tobita.pdf.